Send Orders for Reprints to reprints@benthamscience.ae

Recent Patents on Anti-Cancer Drug Discovery, **2017**, *12,* **000-000**

RESEARCH ARTICLE

Molecular Modelling of Berberine Derivatives as Inhibitors of Human Smoothened Receptor and Hedgehog Signalling Pathway Using a Newly Developed Algorithm on Anti-Cancer Drugs

Parham Jabbarzadeh Kaboli[1,*], Mohammad Bazrafkan[2], Patimah Ismail[1] and King-Hwa Ling[1,3]

[1]*Department of Biomedical Science, Faculty of Medicine and Health Sciences, Universiti Putra Malaysia, Serdang 43400, Selangor, Malaysia;* [2]*Department of Pharmaceutical and Pharmacological Sciences, University of Padova, Padua, Italy;* [3]*Genetics and Regenerative Medicine Research Centre, Faculty of Medicine and Health Sciences, Universiti Putra Malaysia, Serdang 43400, Selangor, Malaysia*

Abstract: ***Background***: Protoberberine isoquinoline alkaloids are found in many plant species. They consist of a diverse class of secondary metabolites with many pharmacologically active members, such as different derivatives of berberine already patented. In the development of approximately 20-25% of all cancers, altered hedgehog (Hh) signalling is involved where the smoothened (Smo) transmembrane receptor triggers Hh signalling pathway towards *Gli1* gene expression.

Objective: The current study aimed to model and verify the anti-Smo activity of berberine and its derivatives using a novel automated script.

Method: Based on the patented inventions filed on ADMET modelling until 2016, which also predicts ADMET parameters and binding efficiency indices for all molecules, a script was developed to run automated molecular docking for a large number of small molecules.

Results: Berberine was found to interact with Lys395 of Smo receptor via hydrogen bonding and cation-π interactions. In addition, π-π interactions between berberine aromatic rings and two aromatic residues in the Smo transmembrane domain, Tyr394 and Phe484, were noted. Binding efficiency indices using an *in silico* approach to plot the Smo-specific binding potency of each ligand was performed. The mRNA level of *Gli1* was studied as the outcome of Hh signalling pathway to show the effect of berberine on hedgehog signalling.

Conclusion: This study predicted the role of berberine as an inhibitor of Smo receptor, suggesting its effectiveness in hedgehog signalling during cancer treatment.

ARTICLE HISTORY

Received: April 29, 2017
Revised: July 23, 2017
Accepted: September 25, 2017

DOI:
10.2174/1574892812666170929131247

Keywords: Berberine, cancer, cyclopamine, hedgehog signalling pathway, molecular dynamics simulations, molecular modeling, smoothened receptor.

1. INTRODUCTION

Altered hedgehog (Hh) signalling is involved in the development of approximately 20-25% of all cancers. The absence of a ligand, PTCH1 and PTCH2 can inhibit downstream signalling by antagonising the function of the Smoothened transmembrane (TM) receptor (Smo) [1]. Somatic mutations in Smo have been identified in sporadic basal cell carcinomas (BCC) and medulloblastoma. Somatic gain-of-function mutations in *Smo* reported in meningiomas are believed to increase tumorigenesis through over-activation of Hh signalling. The mutated Hh pathway is also associated with blood malignancies [2, 3] and breast cancer [4].

*Address correspondence to this author at the Department of Biomedical Science, Faculty of Medicine and Health Sciences, Universiti Putra Malaysia, Serdang 43400, Selangor, Malaysia; Tel/Fax: +60 1-4261-4574; E-mail: parham@gromacs.net

Cyclopamine, a plant-derived steroidal alkaloid, binds directly to the TM helices of Smo, inhibiting Hh signalling. The discovery of patented small molecule antagonists of SMO [5], like cyclopamine, has opened up exciting prospects for targeted therapy and prevent cancers associated with Hh signalling [6]. Other synthetic inhibitors of Smo, such as CUR61414, have also been reported to effectively reduce BCC. The CUR61414 has been tested against BCCs in a Phase I clinical trials. Recently, more than 50 compounds that inhibit Smo were identified [7-13]. In most cell lines used to examine molecular mechanisms of Hh signalling, Smo antagonists have inhibitory concentrations (IC_{50}) of around 300nM or less [14-16]. Cyclopamine, at high doses (≥ 10μM), however, has been shown to inhibit growth of a subset of breast cell lines *in vitro* [4]. To date, the most clinically studied anticancer agent is vismodegib (GDC-0449), which was approved by the US Food and Drug Ad-

1574-8928/17 $100.00+.00

ministration for the treatment of BCC [17]. Another drug approved for BCC treatment is sonidegib (LDE225) [18], effective for taxane-mediated chemoresistance in ovarian cancer [19].

According to the Universal Protein Resource, the human Smo receptor contains 787 amino acids (Uniprot ID: Q99385). It has three main domains: an extracellular domain (ECD; residues 1-191), a heptahelical TM domain (7-TM; residues 224-534), and a cytoplasmic domain (residues 535-787) [20]. When the Smo receptor's side chain is perpendicular to the main 7-TM axis, its activity stops in the middle of the helical bundle, forcing the bound antagonist to interact with extracellular loop residues (e.g., cyclopamine and vismodegib). In contrast, when this side chain is parallel to the main 7-TM axis, a back pocket opens, allowing deeper penetration into a bigger TM cavity (e.g., SANT-1) [20-22].

Inhibiting SMO using vismodegib blocks the transcription of tumour-mediating genes associated with the Hh pathway [23, 24]. However, one patient with a metastatic form of medulloblastoma relapsed after initially responding to the drug due to Smo mutation in the sixth TM helix (D473H) that disrupted vismodegib binding [12, 25]. Furthermore, acquired resistance was also reported in BCC patients undergoing vismodegib treatment [26]. Analysis of resistance mechanisms in a medulloblastoma mouse model treated with sonidegib found that Smo, PI3K, and Gli2 were activated [27]. Therefore, identifying other Smo inhibitors that reduce chemotherapeutic drug resistance when administered as an alternative or combination therapy is of great interest.

The inhibitory effect of berberine (BBR), a plant-based alkaloid, on Smo was first reported by Wang *et al.* (2015) [28], but its mechanism(s) of interaction have not yet been defined, requiring further studies. Thus, the objective of the current study is to measure and verify the inhibitory effects of BBR as Smo inhibitor. Additionally, alternative anti-Smo candidates- among a large number of berberine derivatives as already patented [29]- can be predicted by a new script that we developed to facilitate virtual high-throughput screening of compounds against a specific target. Therefore, the specific objective of this study was to test this script for analysing berberine derivatives against Smo receptor. The script setup was based on BBR and cyclopamine experimental studies.

2. MATERIAL AND METHODS

2.1. Background and Patents on Virtual HTS/ADMET Modelling

AutoDock is a popular non-commercial docking program [30]. It implements Lamarckian genetic algorithm (LGA) for computing conformations [31], simultaneously reducing the thermodynamic energy to predict the best conformations of the ligands against the enzyme of interest [32]. However, pharmacologists have the tendency to inspect hundreds of docked structures or molecules with similar basic structures, but which AutoDock does not (specifically, it does not inspect the docking of hundreds of different small molecules against different crystals of one enzyme) [31]. In order to increase the reliability of docking, the number of X-ray crystals of the target and the iterations (repeats) of each docking is increased, and the average is then calculated [32]. In the case of cancer, in order to understand how different small molecules bind to the target for finding the best molecules which therapeutically inhibit the over-activated enzyme or receptor, expensive High-Throughput Screening (HTS) experiments or cheaper virtual High-Throughput Screening (VHTS) must be performed [33]. Raw materials for docking are available on PubChem and RCSB Protein Data Bank (PDB) as they are the most popular databases for small molecules and protein crystal structures respectively [33].

In the case of protein-ligand High-Throughput docking, there are several docking softwares of which electronic High Throughput Screening (eHiTS) is well regarded [34]. It recognises the probable binding site based on the systematic search in contrast to AutoDock, which uses stochastic LGA, both of which lack any prediction in bioavailability and absorption, distribution, metabolism, excretion, and toxicity (ADMET) of the docked compounds [30]. As AutoDock is developed based on single ligand/target docking and only predicts different conformations of one small molecule against one crystal of protein of interest, DOVIS has been developed which uses AutoDock (version 3) as the docking engine and runs on a Linux cluster for a large number of small molecules. In order to prepare a list of the most effective ligands, DOVIS docks large numbers of ligands to an enzyme, and the docking scores are then calculated [35]. As the molecular structure directly affects ADMET properties of ligand, it is important to develop a software which predicts ADMET properties of compounds as well as calculate its docking parameters.

Based on the patented inventions filed on ADMET modelling, a method was developed by which a compound is structurally redesigned to improve one or more of its ADMET/pharmacokinetics properties [36]. This method includes identifying a therapeutic chemical compound based on its chemical structure before a model was developed to determine the most important therapeutic features of the compound. Similarly, another method was developed to predict the therapeutic potency and one or more ADMET properties of all or part of a chemical compound [37]. This method is able to screen libraries of chemical compounds, and reliably identifies small subsets of those chemical compounds that have desirable therapeutic potency and ADMET properties. Unlike these methods which predict ADMET properties based on modelling of other compounds, Abbreviated Profile of Drugs (A-POD) was recently introduced to predict pharmacokinetics properties based on the given compounds [38]. Recently, a method of selecting compounds with reduced risk of cardiotoxicity was introduced [39]. The human Ether a-go-go related gene 1 (hERG1) K+ ion channel has been indicated as an ADMET property involved in cardiotoxicity. Therefore, the recent patent screens compounds based on their inhibitory effects on cardiac ion channel, including hERG1. Accordingly, an enzyme-specific method, ranking compounds based on binding efficiency index, has likely greater impact in developing anti-cancer drugs.

Binding Efficiency Indices (BEIs) are calculated to optimise the thermodynamics of docking based on the physico-

chemical properties of each ligand. Two types of information are vital here: (1) molecular properties of ligands, such as molecular weight (MW), topological polar surface area (TPSA), LogP, number of heavy atoms, and number of polar atoms (N + O); (2) thermodynamics features resulting from molecular docking, such as binding energy and pK_i. In order to calculate efficiency indices, molecular properties and docking information are combined to provide quantitative parameters showing the specificity of each compound to target protein. Abad-Zapatero's formulas and definitions are used to calculate the BEIs [40].

In order to maximise the predictability of potential drug candidates, an application was developed which not only runs automated molecular docking for a large number of small molecules using AutoDock, AutoDock Vina, and BetaDock, but it also predicts ADMET parameters and binding efficiency indices for all docked molecules [41]. To run this algorithm, only a bash command under Linux platform is required and a CSV-formatted Microsoft Excel file containing a sorted list of all docked compounds is generated. Both script and final list of compounds are available on the online version of this article.

2.2. Ligand Selection

Using the PubChem database, virtual screening for all compounds similar to BBR (PubChem CID: 2353; DrugBank ID: DB04115; ZINC ID: 03779067) was done. A total of 1544 similar compounds were identified and sorted based on their chemical properties (MW, hydrogen bond donor, hydrogen bond acceptor, formal charge, total formal charge, calculated LogP, etc.). Lipinski's rule of 5 was checked for all BBR-like compounds, and 485 ligands passed the rule of 5 (Table **1** and Fig. **1**).

2.3. Crystals of SMO Receptor

Using the RCSB Protein Data Bank [42], four crystal structures of the Smo TM domain were downloaded (PDB IDs: 4n4w, 4o9r, 4qin, and 4jkv), and ligands were docked to all Smo crystals to perform four independent *in silico* experiments (Table **2**). As experimental conditions of crystallography are different, four different crystals of Smo were used to compare the results and calculate the average for each docking parameter.

2.4. Grid Box Determination for Docking

In order to determine the CA atom of Asn219, the 4o9r structure co-crystallised with cyclopamine was used and redocked with the latter to evaluate the ability of AutoDock to identify the real binding pose of cyclopamine (as shown *in silico* positive control). The root-mean-square deviation (RMSD) was acceptable amount of 2.90 Å and the residue Asn219 formed H-bond with cyclopamine. Therefore, Asn219 at CA atom was selected as the centre of grid box throughout this study. Docking and genetic algorithm setup was done based on previous studies [32].

MD Simulations

All MD simulations were done using GROMACS v.5.0.4 under Ubuntu Linux platform v.15.0.4, with the GROMOS 53a6 force field provided by Automated Force Field Topology Builder v. 2.2 [43]. Water systems were generated so that each docked protein was placed in the centre of a triclinic box with a minimum distance between the solutes and box edge of 1.0nm. Accordingly, all solutes were solvated using SPC water model [43]. The systems were then neutralised by adding sodium and chloride ions.

Energy was minimised using the steepest descent algorithm until the maximum force was lower than 1000kJ/mol·nm on any atom, and the maximum number of minimisation steps was adjusted to 50,000 with an energy step size of 0.01. Simulation was done with Particle-Mesh Ewald electrostatics, using a cubic interpolation order and with a Fourier spacing of 0.16nm. Before starting the final MD run, two equilibration stages in NVT and NPT ensembles were conducted. First, the temperature during simulation was adjusted to 300K, and the system was then equilibrated using a modified Berendsen velocity rescaling thermostat [44]. Pressure during isothermalisobaric ensemble (NPT) was adjusted to 1 bar using a Parrinello-Rahman barostat [45]. The simulation length was 300ps in each equilibration stage with a simulation time step of 2.0fs [46]. A cut-off set to 1.4nm was used for both van der Waals interactions and the short-range Particle-Mesh Ewald electrostatic component. The cut-off distance of the short-range neighbour list was 1.4nm, and the list updated every 10 steps. The same configurations, including energy minimisation, NVT, and NPT stages, were used for the best-docked targets, and finally, 10ns MD simulations were carried for different Smo receptors. 10ns MD production runs were performed for well-docked proteins.

2.5. Molecular Visualization

Intermolecular interactions were demonstrated using Accelrys Discovery Studio Visualizer v.4.1. In addition to Discovery Studio, intermolecular hydrogen bonds were also checked by LigPlot$^+$ v.1.4.5 and UCSF Chimera v.1.10.2 [47].

2.6. *In vitro* Material

MCF-7 breast cancer cell line was gifted by Prof. Johnson Stanslas, the pharmacotherapeutics laboratory (FMHS, UPM). To grow the cells in 25Cm^2 flask (690195, Greiner Bio-One, Germany), RPMI 1640 media (R8758-500ML, Sigma, USA), fetal bovine serum (F7524-100ML, Sigma, USA), Penicillin-Streptomycin (P0781-20ML, Sigma, USA), Phosphate buffered saline tablet (PBS) (P4417, Sigma, USA), Trypsin-EDTA solution (T3924-100ML, Sigma, USA), and epidermal growth factor (E41271MG, Sigma, USA) were used. To do apoptosis assay, TACS Annexin V-FITC Apoptosis Detection Kit (Trevigen, 4830-01-K) and to perform cytotoxicity (MTT) assay, 3-(4,5-dimethyl-2-thiazolyl)-2,5-diphenyl-2H-tetrazolium bromide (M5655, Sigma, USA) and standard proliferation assay kit II (ab65475, Abcam) were used. Berberine (B3251, Sigma-Aldrich, Canada), SAG (4366, Tocris Bioscience), and cyclopamine (1623, Tocris Bioscience) were purchased. cDNA synthesis and qPCR kits were purchased from Qiagen (208052, 249900).

Table 1. Molecular Properties of the Top Thirty Berberine (BBR) Derivatives Plus Berberine against SMO Receptor. The full list is Available as Supplementary File.

Rank	PubChem CID	MW(kDa)	NHA	nHBD	nHBA	nTDOF	N+O	TPSA	LogP	Molecular Formula
1	76021944	0.484475	35	4	9	8	10	130.95	0.268	$C_{25}H_{26}NO_9^+$
2	58033315	0.363387	27	1	5	5	6	67.04	3.5068	$C_{21}H_{19}N_2O_4^+$
3	46906833	0.469509	35	1	5	6	7	69.9	4.5683	$C_{28}H_{25}N_2O_5^+$
4	53357841	0.484475	35	4	9	8	10	130.95	0.268	$C_{25}H_{26}NO_9^+$
5	50899703	0.45651	34	0	5	6	6	50.03	4.8131	$C_{28}H_{26}NO_5^+$
6	67699535	0.374475	28	0	4	5	4	34.59	4.5579	$C_{24}H_{26}N_2O_2$
7	57580963	0.462494	33	0	6	4	7	83.32	4.9362	$C_{25}H_{20}NO_6S^+$
8	77338459	0.374475	28	0	4	5	4	34.59	4.5579	$C_{24}H_{26}N_2O_2$
9	73352427	0.477572	35	0	6	8	7	53.27	3.9069	$C_{28}H_{33}N_2O_5^+$
10	44511311	0.485574	36	0	5	7	7	47.92	3.9103	$C_{29}H_{31}N_3O_4^{+2}$
11	11682783	0.365402	27	1	5	5	6	66.82	3.1255	$C_{21}H_{21}N_2O_4^+$
12	44583275	0.447546	33	0	5	6	6	44.04	4.2804	$C_{27}H_{31}N_2O_4^+$
13	76021905	0.484475	35	4	9	8	10	130.95	0.2664	$C_{25}H_{26}NO_9^+$
14	52944636	0.433519	32	0	5	5	6	44.04	3.8903	$C_{26}H_{29}N_2O_4^+$
15	52948350	0.433519	32	0	5	6	6	44.04	3.8903	$C_{26}H_{29}N_2O_4^+$
16	44429431	0.438539	32	2	6	12	7	92.84	4.2234	$C_{25}H_{32}N_3O_4^+$
17	53357839	0.484475	35	4	9	8	10	130.95	0.2664	$C_{25}H_{26}NO_9^+$
18	76315363	0.426439	31	3	7	9	8	101.49	1.1806	$C_{23}H_{24}NO_7^+$
19	44583330	0.442506	33	0	4	6	6	44.68	3.8443	$C_{27}H_{26}N_2O_4^{+2}$
20	44583272	0.460497	34	0	5	6	6	44.68	3.9834	$C_{27}H_{25}FN_2O_4^{+2}$
21	53341157	0.483535	36	1	5	7	7	69.9	4.9584	$C_{29}H_{27}N_2O_5^+$
22	46906895	0.42848	32	0	4	5	6	44.68	3.4542	$C_{26}H_{24}N_2O_4^{+2}$
23	73352429	0.479545	35	0	7	8	8	62.5	2.7532	$C_{27}H_{31}N_2O_6^+$
24	71537339	0.456513	34	0	6	4	7	66.58	4.3819	$C_{27}H_{26}N_3O_4^+$
25	44583336	0.457498	34	0	6	7	7	62.92	4.3306	$C_{27}H_{25}N_2O_5^+$
26	44583270	0.456533	34	0	4	6	6	44.68	4.1527	$C_{28}H_{28}N_2O_4^{+2}$
27	44583342	0.473501	35	1	5	7	9	101.71	3.2769	$C_{26}H_{25}N_4O_5^+$
28	49870985	0.493575	36	2	8	12	9	121.94	3.8305	$C_{27}H_{32}N_4O_5$
29	53357698	0.484475	35	4	9	8	10	130.95	0.2664	$C_{25}H_{26}NO_9^+$
30	427682	0.418485	31	0	6	8	6	62.7	4.9927	$C_{25}H_{26}N_2O_4$
184	2353 (BBR)	0.33636	25	0	4	2	5	40.8	3.0963	$C_{20}H_{18}NO_4^+$

MW, Molecular Weight (kilo Dalton); **NHA**, Number of Heavy Atoms (non-hydrogen atoms); $\mathbf{n_{HBA}}$, Number of Hydrogen Bond Acceptors; $\mathbf{n_{HBD}}$, Number of Hydrogen Bond Donors; $\mathbf{n_{TDOF}}$, Number of Torsional Degrees of Freedom; **N+O**, Number of Polar Atoms; **TPSA**, Topological Polar Surface Area.

Table 2. RSCB Protein Data Bank (PDB) Files and Related Information.

PDB ID	Domain	Phenotype	Resolution (Å)	R-value work	R-value free
4n4w [57]	TM	Wild (D473)	2.8	0.204	0.253
4o9r [59]	TM	Wild (D473)	3.2	0.232	0.278
4qin [57]	TM	Wild (D473)	2.6	0.225	0.260
4jkv [57]	TM	Wild (D473)	2.45	0.20	0.231

SMO, Smoothened Receptor; **TM**, Transmembrane Domain; **Wild**, Wild-Type.

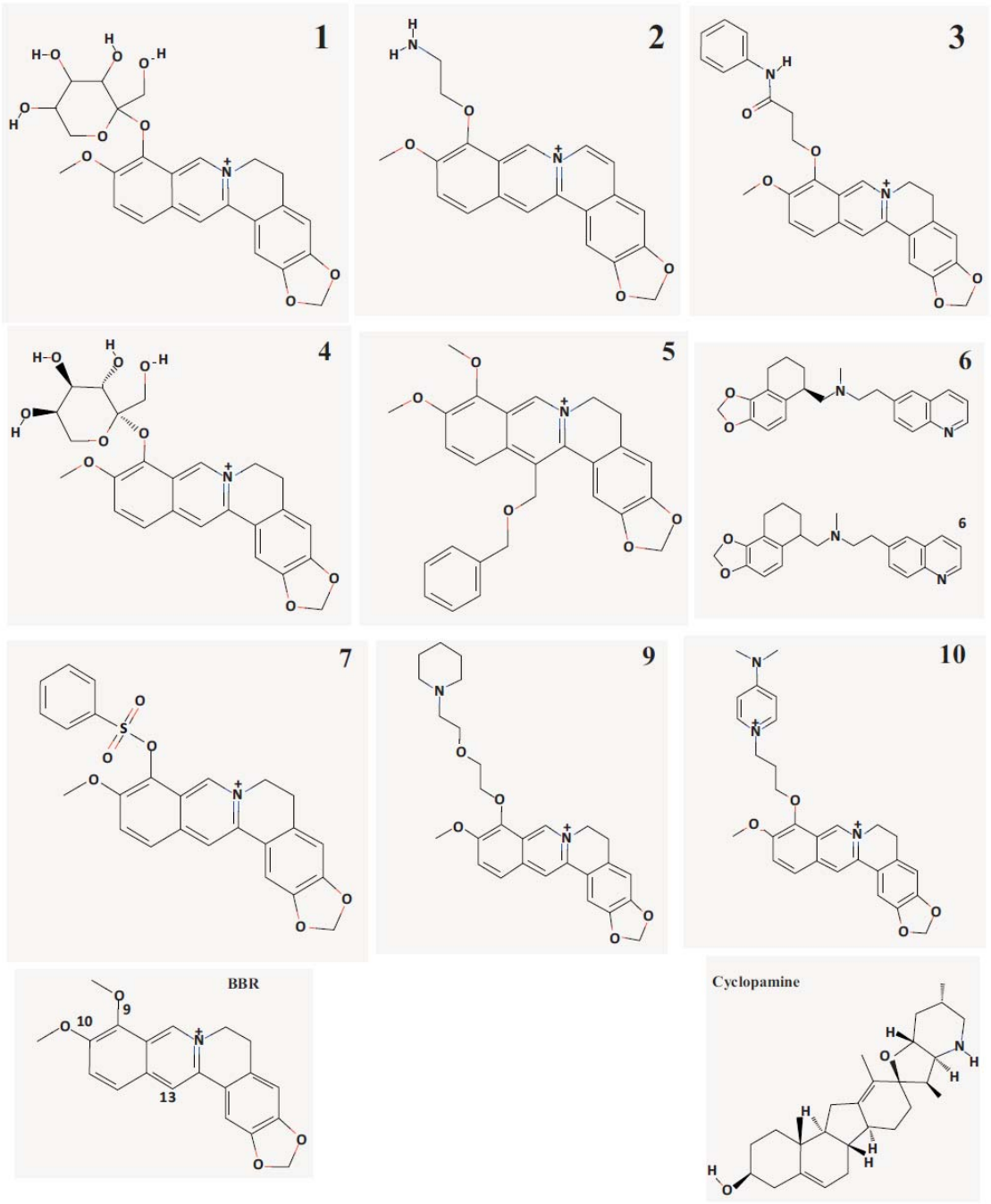

Fig. (1). Berberine structure and top ranked compounds which were included in the present article.

2.7. Cell Culture

MCF-7 cell line was grown in RPMI-1640. Then cell cultures were supplemented with 5% to 10% Fetal bovine serum (FBS), and 1% penicillin-streptomycin using 25cm^2 flasks in a 37° incubator with 5% CO_2 (Wang *et al*., 2009). The cells were then treated with berberine at different doses for 24-72 hours to identify the half maximal inhibitory concentration of drugs.

2.8. Cytotoxicity Assay

In the current study, berberine chloride has been purchased from Sigma-Aldrich and two cell lines were studied. For each cell line, six 96-well plate cultures were seeded by cells (40000 cells/well). Then cultures were treated by different concentrations of berberine chloride at serial concentrations of 0, 3.125, 6.25, 12.5, 25, and 50μM and were maintained at 37°C with CO_2 for three time dependent treatment (24, 48, and 72 hours). According to the standard proliferation assay kit II provided by Abcam (ab65475) cell viability and half inhibitory concentration (IC_{50}) have been measured. The concentration-response curve was then generated for each ligand which is reported. The experiments were repeated three times. For each concentration, three wells were used to do triplicate experiments. To perform MTT assay, 200μl of media containing cells added to each well to have 20000-40000 cells per well, 100μl of media were added to each well except column two, 100μl of drug/media (100μM) were added to column two and three, serial dilutions were prepared from column three. MTT (0.05g) was solved in 10ml of PBS. After treatment incubations, 200μl of fresh media were transferred to each well, and then 50μl of prepared MTT (in dark) were transferred to each well. After a 4h incubation, 200μl of DMSO were added to each well (Shaking). The cell viability was measured by OMEGA BMG LABTECH at 550nm.

2.9. Apoptosis Assay

Annexin V-FITC Apoptosis Detection kit has been purchased from Trevigen. Quantification of apoptotic cells will be determined by Annexin V-FITC/PI staining. The adherent cells were collected by centrifugation and then they were resuspended in 500μl 1 × binding buffer. Then they were stained with 5μL Annexin V-FITC and 5μL propidium iodide (PI) (50μg/mL). For each treatment, a flask with at least 200000cells/ml was seeded. Treatment was performed. In addition to the treatments, three additional flasks should be seeded as controls to configure the Flow Cytometry Machine. For each sample, triplicates were also seeded.

2.10. RNA Extraction and qPCR for GLI and GUSB

Total RNA was extracted from MCF-7 breast cancer cell line using Trizol reagent. *GLI1* (GCID: GC12P057460) was used for quantitative polymerase chain reaction (RT-qPCR). In order to normalize mRNA levels of *GLI1* gene, β-glucuronidase mRNA level (*GUSB*; GCID: GC07M065960) was used following manufacturer's instruction (Qiagen; Catalogue numbers: 208052, 249900).

3. RESULTS

3.1. Docking Information

The present study screened 485 BBR derivatives to study their drug-like properties. Docking analysis was performed on compounds which passed Lipinski's rule of five. For each ligand, four crystals and 30 runs were used for the docking algorithm. The aim of molecular docking was to find out whether BBR and/or its derivatives can bind to Smo, and to determine how close pKi of BBR derivatives is to that of cyclopamine. To calculate pK_i ($-LogK_i$), the average K_i for each ligand was used; a K_i less than 1μM was considered excellent, though a K_i less than 10μM was also acceptable (Table **3**).

Clusters containing a higher number of conformations were determined to be the best. Ligands with large side chains, such as compounds 16, 28 and 1, have a higher range of conformational diversity, indicating a higher number of clusters. The BBR has a lower number of clusters, demonstrating a more rigid ligand conformation, resulting in less K_i variation (Table **3**). Due to the size and structure of the docking cavity in Smo, n_{TDOF} plays a major role in increasing the number of conformations. A higher n_{TDOF} means a higher torsional free energy; hence, the torsional free energy has a positive value (or 0 for cyclopamine). Interestingly, the pK_i of BBR and cyclopamine were 6.30 and 6.60 respectively. A total of 33 BBR derivatives were predicted to have higher pKi than cyclopamine (Table **3**).

3.2. SMO-Ligand Interactions

By visualising docking log files (Figs. **2** & **3**), the interactions made by the ligands in four crystal structures of Smo were compared to find the best position and most frequent ligand conformation. Since hydrogen bonding with a $\Delta G°$ between -3 and -5 kcal/mol removes one donor and one acceptor moiety from the molecule, it increases the hydrophobicity of the docking cavity. The comparison showed Lys395 was involved in several kinds of interactions, including hydrogen bonding and cation-π interactions. Besides hydrogen bonding, a cation-π interaction with a $\Delta G°$ between -1 and -5 kcal/mol was produced by the positively-charged lysine and BBR aromatic group.

Furthermore, aromatic amino acids Phe484 and Tyr394 in the docking cavity interacted with BBR via hydrophobic π-π interactions. Cation-π and π-π interactions increased the binding efficiency of the ligand. Several aromatic rings in the BBR structure not only hydrophobically interacted with Lys395, Tyr394, and Phe484 of Smo, these rings also provided the negative charges to make π interactions with those residues. Lys395 produces hydrophobic π-alkyl and cation-π interactions because of its long alkyl chain and terminal positive charge respectively. Lys395 also has the potential to hydrogen bond with BBR. A lack of any flexible side chain on BBR is beneficial for docking to Smo because its rigid structure will not allow higher torsional changes.

This feature suggests it is an effective ligand for small, hydrophobic Smo cavities. The results obtained from molecular docking of 485 BBR derivatives and four different Smo crystals (Fig. **4**) herein demonstrated that BBR

Table 3. Human Smoothened Receptor (Smo) Docking Information for Top Ranked BBR Derivatives. Selected Berberine (BBR) Derivatives and Cyclopamine, a Well-Known Inhibitor of Smo, were Docked to Four Different Smo Receptors. Sorting and Ranking have been Performed Based on Size-Dependent Binding Efficiency Index (nBEI).

Rank	PubChem CID	Min. E (kCal/mol)	Mean E (kCal/mol)	Min. Ki (nM)	Mean Ki (nM)	pKi	nBEI	NSEI	LLE
1	76021944	-11.98	-11.822	1.65	2.32	8.634512	10.17858	0.863451	8.366512
2	58033315	-12.15	-11.79	1.24	2.487	8.604324	10.0356	1.434054	5.097524
3	46906833	-12.39	-11.662	0.821	3.71	8.430626	9.974665	1.204375	3.862326
4	53357841	-12.33	-11.56	0.91	5.347	8.27189	9.815917	0.827189	8.00389
5	50899703	-12.23	-11.41	1.09	7.115	8.147825	9.679304	1.357971	3.334725
6	67699535	-11.76	-11.295	2.41	6.117	8.213462	9.660584	2.053365	3.655562
7	57580963	-11.53	-11.167	3.53	7.365	8.132827	9.651341	1.161832	3.196627
8	77338459	-11.36	-11.202	4.72	6.275	8.202386	9.649544	2.050597	3.644486
9	73352427	-11.67	-11.17	2.79	9.122	8.03991	9.583954	1.148559	4.13301
10	44511311	-11.92	-11.077	1.82	10.037	7.998396	9.554677	1.142628	4.088096
11	11682783	-12.18	-11.452	1.19	8.022	8.095717	9.527054	1.349286	4.970217
12	44583275	-11.61	-11.052	3.1	9.82	8.007889	9.526402	1.334648	3.727489
13	76021905	-11.69	-11.042	2.72	11.92	7.923724	9.467792	0.792372	7.657324
14	52944636	-11.12	-10.845	7.09	11.672	7.932855	9.437986	1.322142	4.042555
15	52948350	-11.6	-10.917	3.13	12.185	7.914174	9.419324	1.319029	4.023874
16	44429431	-12.13	-11.057	1.29	12.372	7.90756	9.412693	1.129651	3.68416
17	53357839	-12.54	-11.495	0.644	13.831	7.859146	9.403191	0.785915	7.592746
18	76315363	-11.94	-11.045	1.78	14.67	7.83357	9.324932	0.979196	6.65297
19	44583330	-11.24	-10.722	5.76	17.745	7.750924	9.269438	1.291821	3.906624
20	44583272	-11.22	-10.795	5.92	18.455	7.733886	9.265365	1.288981	3.750486
21	53341157	-11.97	-11.185	1.69	19.915	7.70082	9.257122	1.100117	2.74242
22	46906895	-10.8	-10.492	12.15	23.6	7.627088	9.132238	1.271181	4.172888
23	73352429	-10.71	-10.417	14.11	26.517	7.576476	9.120535	0.947059	4.823276
24	71537339	-11.2	-10.517	6.15	26.222	7.581334	9.112805	1.083048	3.199434
25	44583336	-10.63	-10.34	16.15	31.927	7.495842	9.027314	1.070835	3.165242
26	44583270	-11.37	-10.58	4.63	32.432	7.489026	9.020498	1.248171	3.336326
27	44583342	-11.05	-10.365	8.01	36.017	7.443492	8.987554	0.827055	4.166592
28	49870985	-12.06	-10.862	1.45	37.1	7.430626	8.986929	0.825625	3.600126
29	53357698	-11.58	-10.565	3.28	38.302	7.416779	8.960841	0.741678	7.150379
30	427682	-10.8	-10.305	12.17	36.982	7.43201	8.923365	1.238668	2.43931
34	Cyclopamine	-12.86	-9.02	0.37	251.93	6.60	8.08	2.2	2.95
184	2353 (BBR)	-9.47	-8.717	114.29	503.227	6.298236	7.696176	1.259647	3.201936

E, Binding Energy (kcal/mol); $\mathbf{K_i}$, Inhibition Constant (nM); **pKi**, $-\text{Log}K_i$; Number of Independent *in silico* Experiments = 4; $\mathbf{pK_i}$ = $-\text{Log}K_i$ (M); **nBEI**, Binding Efficiency Index per Logarithmic Number of Nonhydrogen Atoms [pK_i+Log(nha)]; **NSEI**, Surface Efficiency Index per Polar Atom, [pK_i/(N+O)]; **LLE**, Ligand Lipophilicity Efficiency (pK_i–LogP).

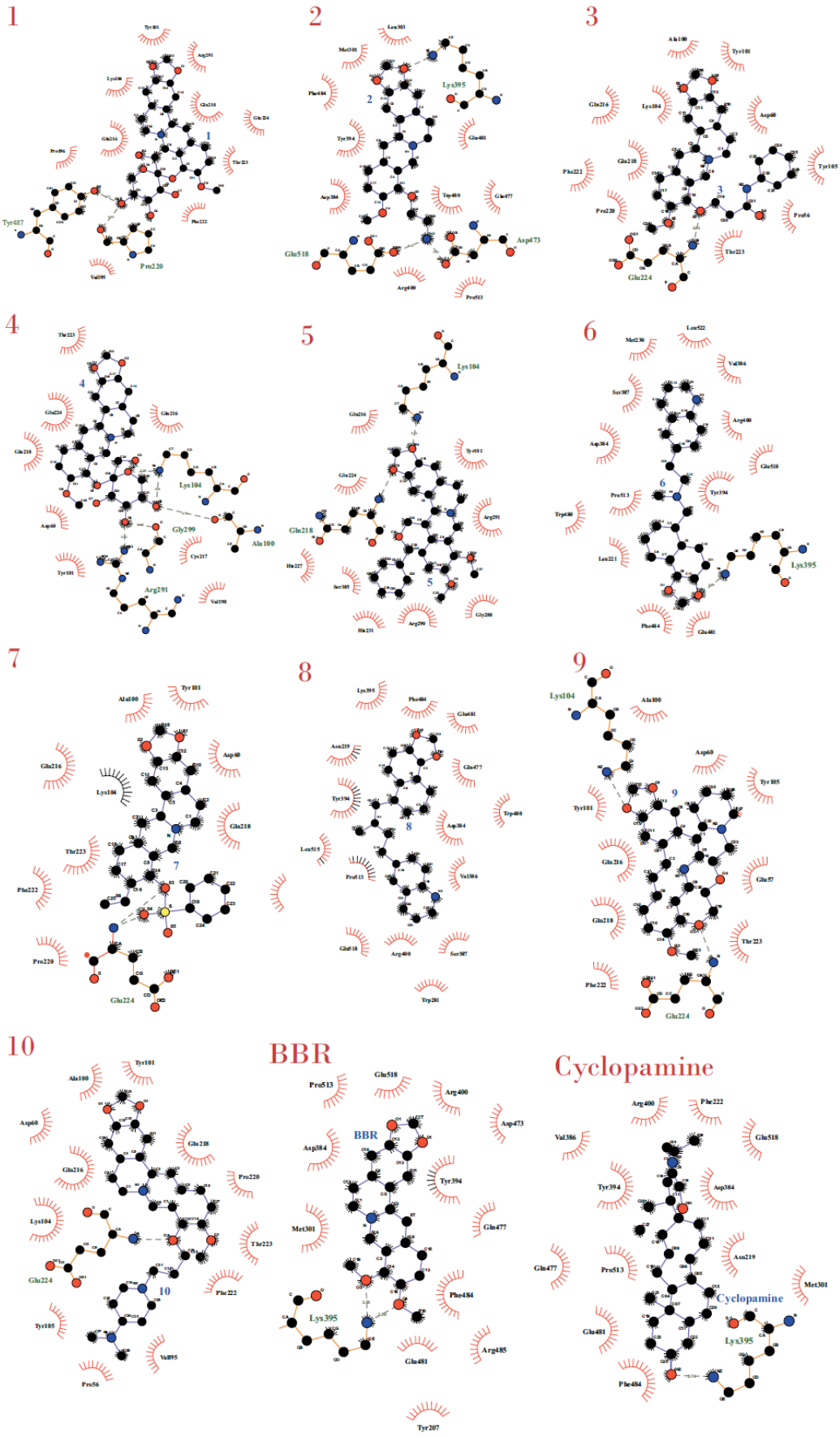

Fig. (2). Interaction between top compounds and the neighboring residues in Smo receptor. Simplified images depicted by LigPlot^{+}.

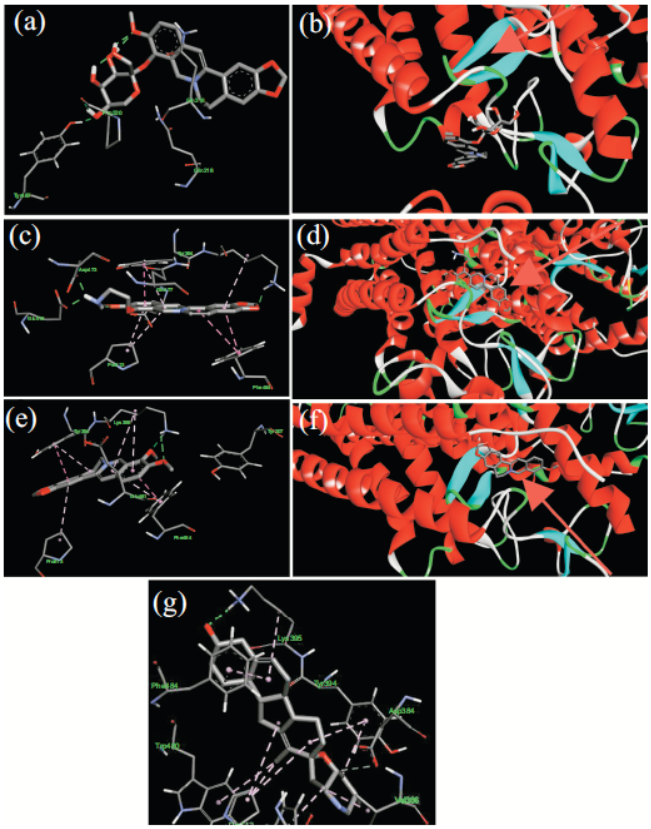

Fig. (3). The most potent inhibitors docked to smoothened receptor. (a-b) Compound 1. **(c-d)** Compound 2. **(e-f)** BBR. Molecular interactions were visualized using Discovery Studio (DS). Lys395 is the most important residue forming a hydrogen bond (green lines) and cation-π interaction. The Phe484 and Tyr394 are involved with π-π interactions (purple lines) between the aromatic rings. Based on the larger size of the molecule, compound 1 was not properly bound to the similar position as BBR and Cyclopamine. Arrows show the correct position above the parallel beta sheets.

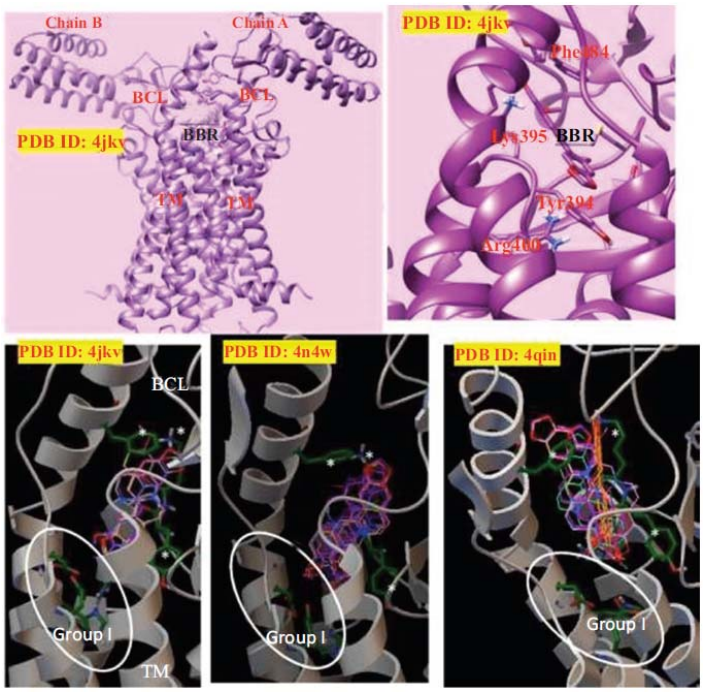

Fig. (4). Comparison of four different Smo crystals marked by their PDB IDs. Thirty concurrent docking conformations are shown for each crystal, as well as the two groups of residues involved with docking. Structural residues including Arg400, His470, Asp473, and Glu518 (Group I) provide a hydrogen binding network needed for the best Smo conformation. Asterisks (*) indicate the second group of residues (Group II) involved in docking (Lys395, Tyr394, and Phe484). Indeed, berberine is trapped between the two groups of residues: ECL: extracellular domain linker; TM: transmembrane domain.

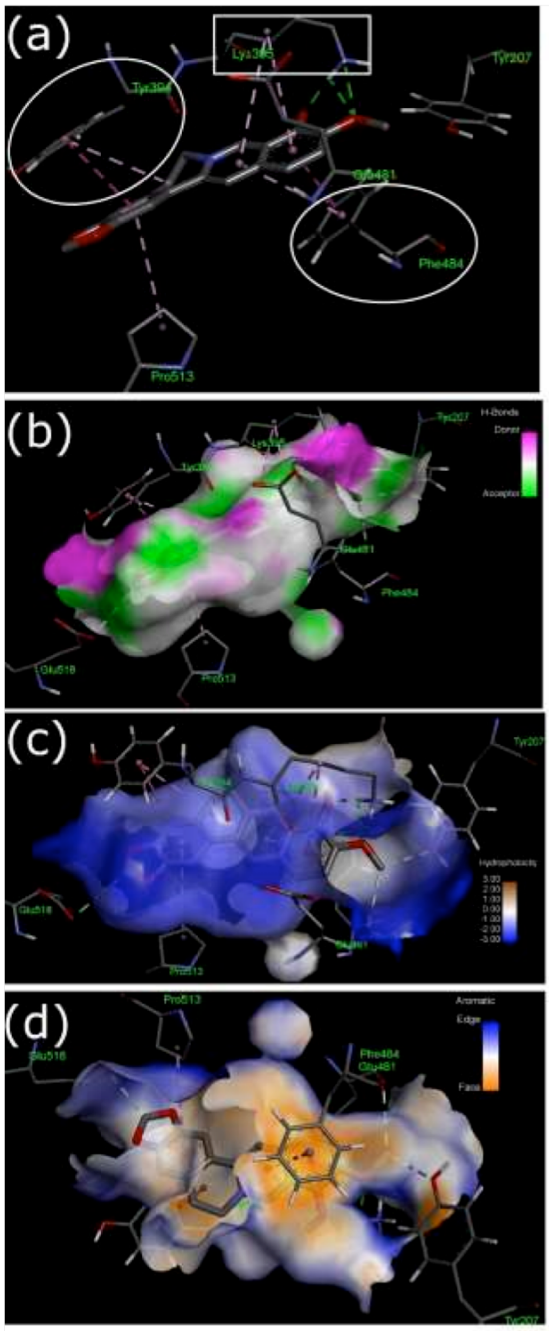

Fig. (5). Berberine/Smo interactions. (a) Tyr394 and Phe484 residues produce π-π interactions with berberine aromatic rings and Lys395 form H-bonds. **(b)** Lys395 forms H-bond through H-bond donors (pink color). **(c)** Smo binding cavity is polar (blue color) where Glu481, Glu518, Lys395, and Tyr394 are in close connections with berberine. **(d)** Phe484 and Tyr394 form face-to-face (orange color) interactions with berberine.

effectively binds the ECD linker via three main interactions: 1) hydrogen bonding, 2) cation-π interaction, and 3) π-π interaction. In several BBR derivatives, the side chains attached to the ligand scaffolds increase the flexibility, polarity and size of the ligands. According to Ma *et al.* (2015), the Smo binding site is narrow and hidden inside the TM helices. Thus, an increase in antagonist size and polarity would decrease its activity [48]. This is confirmed by earlier studies which reported that aliphatic side chains (benzyl and phenyl) reduced the activity of Smo antagonists [7]. We found that adding a large group to three positions on BBR (positions 9, 10, & 13) decreased the pK_i. The rigid structure of BBR containing two methoxy groups was decidedly the best for Smo binding.

It was evident from the four independent *in silico* experiments with 30 repeats each that most of the conformations afforded by docking bound to the ECD linker at the same position (Fig. **4**). The Smo receptor binding pocket depicted in Fig. (**4**) has a long and narrow shape. This pocket was connected to the extracellular aqueous environment via a small opening formed by the ECD linker and a hydrogen bonding network between water and $Arg400^{5.39}$, $His470^{6.52}$, $Asp473^{6.55}$, and $Glu518^{7.38}$ side chains. It is clear that these residues provide electrostatic interactions as well. Therefore, the D473H mutation affects this hydrogen bonding network, resulting in an alteration in the secondary structure of Smo which may have an impact on the effectiveness of the drug. According to Figs. (**4** & **5**), this group of structural residues, called Group I, is located just below the BBR binding site. Furthermore, the residues labelled Group II, trapped BBR by hydrogen bonding and hydrophobic interactions; Lys395 forms the main interactions (hydrogen bond and cation-π), while Tyr394 and Phe484 increase the affinity of BBR by additional hydrophobic interactions.

3.3. Binding Efficiency Metrics

The BEIs were calculated to optimise the thermodynamics of docking based on the physicochemical properties of each ligand using the following information: 1) molecular properties of ligands, such as molecular weight (MW), topological polar surface area (TPSA), LogP, number of heavy atoms, and number of polar atoms (N + O); 2) thermodynamics features resulting from molecular docking, such as binding energy and pK_i. In order to calculate efficiency indices, molecular properties and docking information were combined to provide quantitative parameters, showing the specificity of each compound for the Smo receptor. Then, the chemistry and docking interactions of the different ligands were compared, and bivariate plots were created to determine those which most potently antagonise Smo. nBEI and NSEI efficiency indices measured for BBR were 7.70 and 1.26 respectively, while those of cyclopamine were 8.08 and 2.2 respectively. The formula to calculate each index is found in Fig. (**6**).

Interestingly, while several bivariate plots based on nBEI versus NSEI have been generated, it has been found that 183 BBR derivatives were located at the top of BBR, indicating they were the most potent Smo antagonists with the highest nBEI and NSEI (Fig. **6**). In the linear regression model, the slopes and intercept of the lines are NPOL (N + O) and Log[nha] respectively. Hydrophobicity and polarity of berberine derivatives are provided by aromatic rings and methoxy groups (on position 9 and 10) respectively. Having compared the interactions of the top ranked compounds, it was observed that the docked position is not necessarily the same as previously adjusted positions. In the beginning, docking cavity was

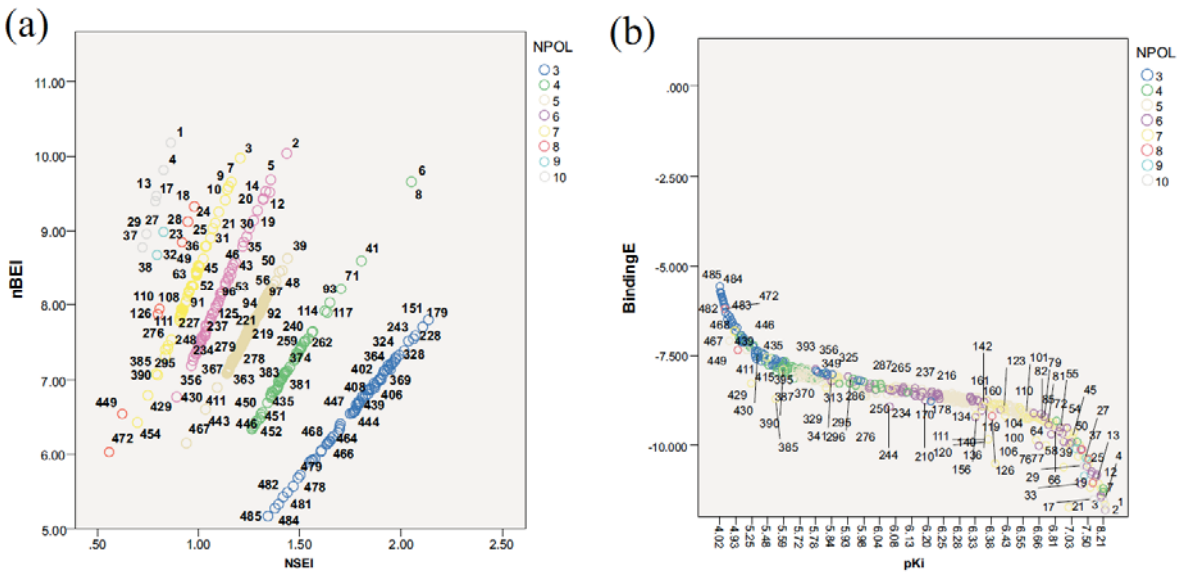

Fig. (6). Optimized bivariate analyses of Smo inhibitors according to binding efficiency indices and molecular properties. Plots demonstrating size- (Y-axis) versus polarity-based (X-axis) parameters. Polarity and size are molecular features which account for bioavailability and ADME of ligands. Size-based indices, such as nBEI, show the lipophilicity whereas polarity-based index such as NSEI, show the hydrophilicity of ligands. The compounds move along the same line in the efficiency plane, upward when gaining in potency and downward when less potent. (**a**) nBEI vs. NSEI. The slopes and intercept of the lines are NPOL (the number of polar atoms) and Log[nha (the number of non-hydrogen atoms or heavy atoms)] respectively; y= NPOL.x + Log[nha]. (**b**) Binding Energy vs. pKi.

predefined by adjusting the centre of grid box before using the docking algorithm. The suitability of molecule for docking is determined by its pKi as well as its size and atomic structure, and accordingly, follow the structure of targeted cavity.

Therefore, the large size of compounds containing the additional sixth ring at the position 9 of BBR (e.g. compound 1) prevents it from properly entering the predefined pocket. According to Fig. (**2**), it can be clearly observed that the residues for compound 2 are similar to those of 184 (BBR) and 34 (cyclopamine). The Lys395 is a key residue that can be seen in cyclopamine/Smo interaction as control; compounds 1, 2, 3 and 5 however, did not dock with the targeted pocket and lacking Lys395. Therefore, because of the small size of the Smo binding pocket, the size of ligands is important. In addition, comparing the visualised interactions of compound 1, 2, and BBR in Fig. (**3**), it has been observed that compound 1 is bound to a different position.

Hence, the much higher nBEI of compound 2 suggests it is a suitable candidate for further evaluation. Meanwhile, BBR is still predicted to be an anti-Smo candidate. Although the compactness and efficiency of compound 2 and Smo receptor are higher than those of BBR and cyclopamine, other factors such as distribution and absorption should be taken into account.

3.4. MD Simulations and Validation

In order to determine the stability of the most potent Smo antagonists (BBR and compound 2) compared with the control ligand (cyclopamine), MD simulations were done. In MD analysis, root-mean-square deviation (RMSD) of simulated docking over time is an appropriate and common criterion used to verify MD simulation stability. For BBR-docked Smo, the average RMSD was lower than that of compound 2. However, the RMSD of compound 2-docked Smo continuously increased (Fig. **7a** & **7d**). Meanwhile, any modification to protein motifs and shape were evaluated by the radius of gyration (Rg). This parameter provides information about the total protein volume distribution in the spherical state; Rg shows molecular shape over time. Rg average for BBR was higher than compound 2 - 3.425nm and 2.86nm for BBR and compound 2 respectively (Fig. **7c** & **7f**). Meanwhile, the average fluctuation for BBR and compound 2 were less than 3Å with the minimum amounts of fluctuation for binding sites (Fig. **7b** &**7e**).

To confirm molecular docking results (Fig. **3**), the number of hydrogen bonds inside Smo after docking of BBR, compound 2, and cyclopamine were 748, 739, and 733 respectively (Table **4**). Interestingly, the average total energies using MD analysis were -1485640, 1486060, and -1485880 kJ/mol for BBR, compound 2, and cyclopamine respectively. Potential and enthalpy were also computed (Table **4**). In order to validate the interactions between Smo and each ligand, radial distribution function (RDF or g(r)) were computed. The RDF shows the distance between the centres of masses of two molecules. BBR was found to have the highest g(r) on the vertical axis [g(r) = 125], matching the radius of 2 Å (Fig. **8a**). The distance of 2 Å shows the effective closeness of the centre of mass of the two molecules. Compound 2 had similar g(r) [g(r) = 125] (Fig. **8b**). Calculation of RDF and other MD parameters clearly established BBR as a new Smo antagonist; the maximal RDF of cyclopamine was 70, at the highest level [g(r) = 70] with a radius of 2 Å (Fig. **8c**).

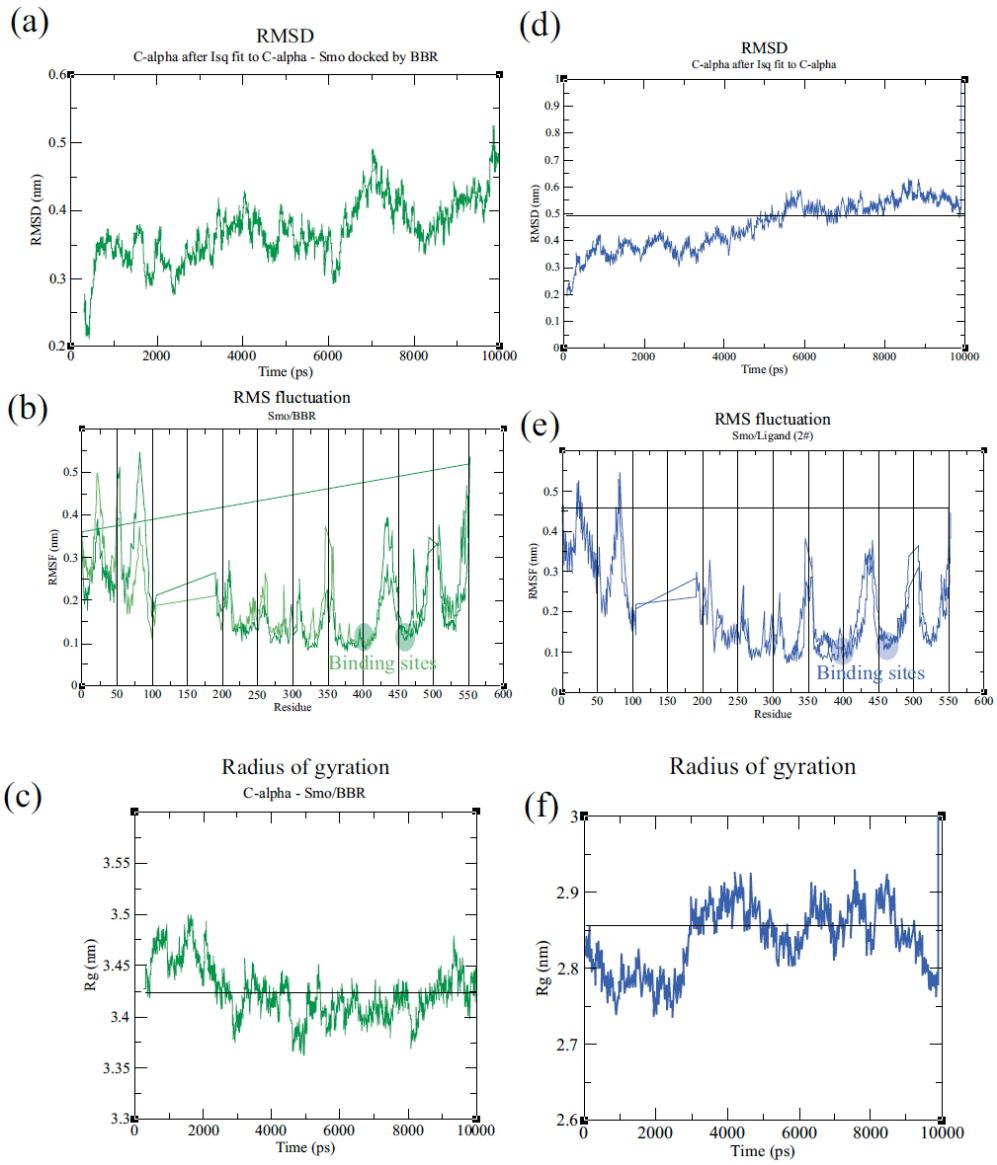

Fig. (7). MD results for the stability of the system after docking of BBR and compound 2. (a-c) Smo/BBR. **(d-f)** Smo/compound 2. The Smo crystal used to generate these charts was 4jkv. The changes of Cα between two states (before and after docking) have been analyzed over times.

Table 4. Energy Computations and the Average Number of HYDROGEN Bonds Provided. The Computations for Two Potent Anti-Human Smoothened Receptor Candidates And Cyclopamine (Positive Control).

Molecular System	Parameter	Average	Err.Est.	RMSD	Tot-Drift	Unit
Smo/184 (BBR)	Potential	-1.8149e + 06	59	-nan	-308.743	kJ mol^{-1}
	Total energy	-1.48546e + 06	59	-nan	-317.869	kJ mol^{-1}
	Enthalpy	-1.48538e + 06	59	-nan	-317.846	kJ mol^{-1}
	Temperature	299.995	0.0058	-nan	-0.00831438	K
	Pressure	0.846786	0.3	-nan	0.8090	Bar
	Hydrogen bonds	747.644	-	-	-	Number
Smo/2	Potential	-1.81552e + 06	81	1505.04	-354.021	kJ mol^{-1}
	Total Energy	-1.48606e + 06	73	1926.42	-284.955	kJ mol^{-1}

Table (4) contd….

Molecular System	Parameter	Average	Err.Est.	RMSD	Tot-Drift	Unit
Smo/2	Enthalpy	-1.48598e + 06	73	1926.45	-284.91	kJ mol^{-1}
	Temperature	299.978	0.011	0.9051	0.0629	K
	Pressure	0.936833	0.51	70.2425	2.31	Bar
	Hydrogen bonds	738.913	-	-	-	Number
Smo/34 (Cyclopamine)	Potential	-1.81535e + 06	57	1484.68	-294.234	kJ mol^{-1}
	Total energy	-1.48588e + 06	59	1905.24	-281.064	kJ mol^{-1}
	Enthalpy	-1.4858e + 06	59	1905.27	-281.082	kJ mol^{-1}
	Temperature	299.986	0.0062	0.896186	0.0119832	K
	Pressure	1.50787	0.096	70.4832	-0.407059	Bar
	Hydrogen bonds	733.186	-	-	-	Number

-nan, not-a-number.

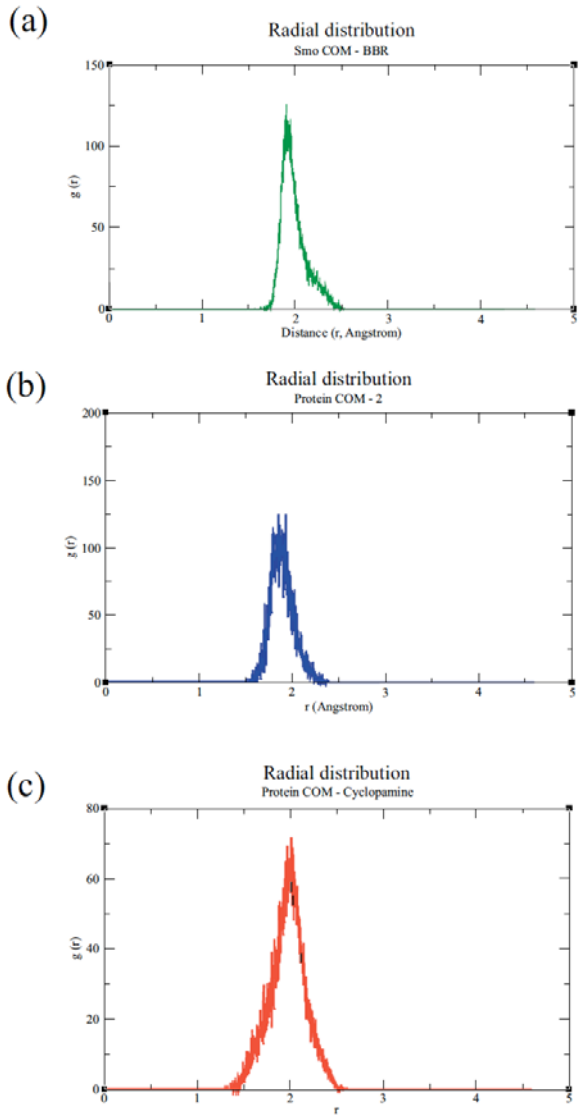

Fig. (8). Results computed for the number of RDF during 10 ns MD simulations. (a) BBR. **(b)** Compound 2. **(c)** Cyclopamine. Cyclopamine used as control compound to observe how the compactness of the system is close to cyclopamine as the confirmed Smo inhibitor.

3.5. BBR Inhibits Hh Signalling in MCF-7 Breast Cancer Cells

Kasper *et al.* showed that Hh signalling can be considered as drug target in breast cancer [49]. In order to study the effect of BBR on breast cancer cells, we have chosen MCF-7 cells. Their toxic effect was first examined (Fig. **9**). Using MTT assay, half inhibitory concentration (IC_{50}) was 12μM after 72h of BBR treatment. Using flow cytometry, BBR also showed different cellular toxicity. After 72h treatment of BBR, apoptotic and necrotic cells were detected. *Gli1* RNA expression is the final outcome of induced Hh signalling. In order to determine how effective BBR is on Hh signalling and to evaluate *in silico* procedure in this study, the levels of *Gli1* RNA expression were measured. First, 5nM of smoothened receptor agonist (SAG) was added to all BBR-containing culture flasks to induce Smo receptor in MCF-7 cells. The normalised levels of *Gli1* expression were calculated with and without SAG as illustrated by Fig. (**9**) (e-f). It was observed that the levels of *Gli1* expression gradually decreased while the concentration of BBR increased. Without using SAG, the RNA levels were almost one-twentieth of SAG-containing cultures. As a positive control, cyclopamine was used as well as SAG to compare the results with BBR-SAG containing flask. As the levels of *Gli1* expression strongly decreased in [SAG+cyclopamine] and [SAG+BBR] cultures, BBR seems to be a competitive inhibitor of Smo.

4. DISCUSSION

Many *in vitro* assays allow measurement of the inhibitory effects of compounds on signalling pathways but they provide little or no information about the underlying target. Smo binding assays have been developed to assess whether the inhibitory effects of certain ligands are mediated by direct or indirect targeting. BODIPY-cyclopamine, a fluorescent derivative of cyclopamine, binds specifically to cells expressing Smo [50]; using a potent anti-Smo candidate can displace BODIPY-cyclopamine by competitive inhibition.

Nevertheless, these *in vitro* methods may not be optimal for determining whether Smo is a direct target of BBR and/or its derivatives because BBR can affect several signalling pathways [51, 52] thus leading to perturbed crosstalk.

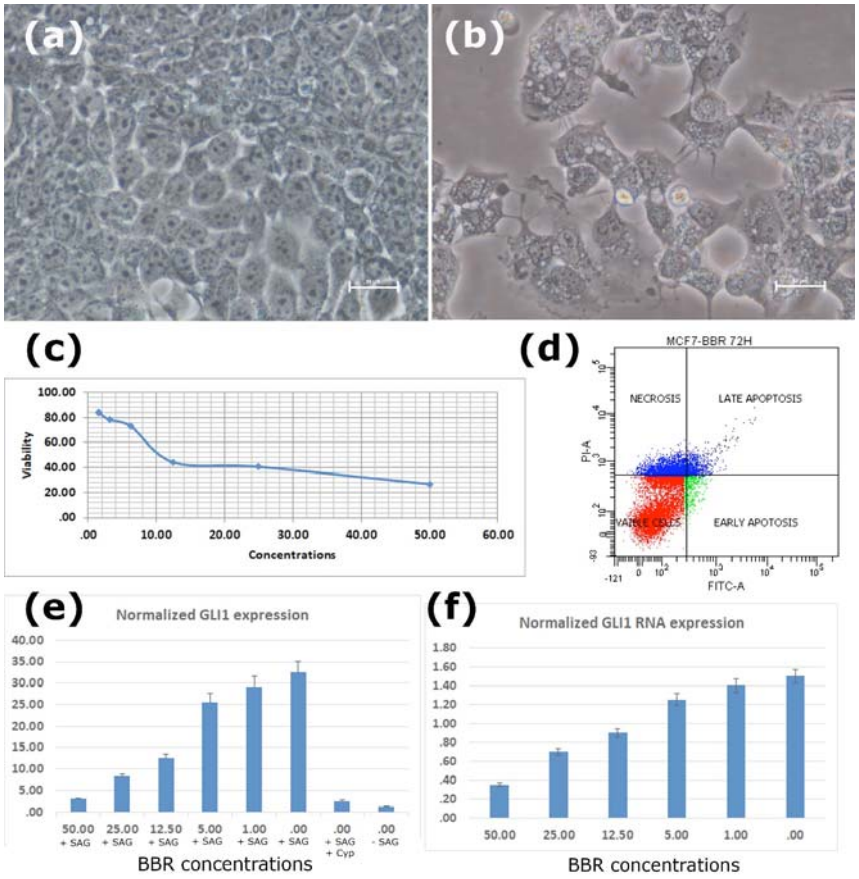

Fig. (9). The effects of BBR on MCF-7 breast cancer cells. (a) MCF-7 untreated breast cancer cells. Scale= 50μm; **(b)** MCF-7 BBR-treated cells (72h) Scale= 50μm; **(c)** MTT results of BBR after 72h of treatment (IC50= 12μM); **(d)** Result of apoptosis assay after 72h of BBR treatment; **(e)** Normalized *Gli1* expression after SAG, BBR, and cyclopamine (Cyp) treatment; **(f)** Normalized *Gli1* RNA expression without SAG treatment.

For example, a reduction in Hh ligands is known to lead to Smo inactivation, and potentially effective crosstalk between Hh signalling and MAP kinase, PI3K, and even Wnt/β-catenin pathways has been demonstrated [53].

Furthermore, *in silico* experiments and related computations are useful for predicting target(s) of small compounds and increase the chances of a demonstrating the accuracy of a tested target *in vitro* evaluations are needed. Earlier X-ray crystallography studies of ligand docked targets, from real biological experiments uploaded to the Protein Data Bank database, enabled researchers to determine the protein conformation most comparable to real experiments. Following this step, the original ligand was removed, and BBR derivatives were replaced prior to conducting molecular docking experiments. The present study also normalised all experiments using a control ligand (cyclopamine) with known biological activity and mechanisms of action against the target (Smo).

Recently, Wang *et al.* (2015) showed the inhibitory effects of BBR on Smo and suggested there might be indirect effects which need further verification [28]. This finding is confirmed by the current study although our data strongly supported BBR as the best Smo inhibitor, the other BBR derivatives investigated should be considered for further *in vitro* and preclinical studies of cancers involving activation of Smo, especially in metastatic cases.

CURRENT & FUTURE DEVELOPMENTS

In conclusion, the study showed that BBR can stably bind and potently inhibit Smo at the same site as cyclopamine, a well-known Smo inhibitor. The MD simulations also demonstrated that the stability of the BBR/Smo interaction is similar to that of cyclopamine and Smo. Although the pKi of BBR is lower than that of cyclopamine, results support BBR as a suitable alternative Smo antagonist. Chemotherapeutic drug resistance evolving from continuous administration of drugs or other factors increases the need for the development of other antagonists. Thus, the BBR has been reported to be effective against various cancer signalling pathways, and studies of specific BBR targets will facilitate development of multi-target, anticancer drugs. Thus, performing these new *in silico* computational strategies on all *in vitro* studies to increase their significance and accuracy is encouraged. Finally, based on the sorted list of BBR derivatives from Virtual High-Throughput Screening, it was found that after chemical synthesis and further evaluation there might be more effective candidates against Smoothened receptor.

The present algorithm is also suitable for performing molecular modelling of a large number of compounds against a specific protein of interest. The rapid performance is timely important, and its reliability is based on previous experiments reported on PubChem database. Therefore, the outcome is of a prediction based on both *in vitro* and *in silico*

data. Its performance, however, is required to be improved for the analysis of millions of compounds for which the current algorithm does not properly work. Currently, the running time highly depends on the number of processors, and increases to several weeks while thousands of molecules are being analysed by current quad-core lap tops. Therefore, the script can be improved so that detects the processors and automatically configures the running speed based on the performance of computers.

LIST OF ABBREVIATIONS

ADMET	=	Absorption, Distribution, Metabolism, Excretion, and Toxicity
ATB	=	Automated Topology Builder
BBR	=	Berberine
BEI	=	Binding Efficiency Index = $\frac{pKi}{MW}$
DS	=	Discovery Studio
EM	=	Energy Minimization
Err.Est.	=	*Error Estimate*
FF	=	Force Field
Gromacs	=	GROningen Machine for Chemical Simulations
GROMOS	=	GROningen Molecular Simulation Computer Program Package
HBA	=	Hydrogen Bond Acceptor
HBD	=	Hydrogen Bond Donor
Ki	=	Inhibition Constant
LLE	=	Ligand Lipophilicity Efficiency Index = pKi - $LogP$
LogP	=	Logarithm of Partition Coefficient
MD	=	Molecular Dynamics
μM	=	Micromolar, 10^{-6} Molar
μm	=	Micrometer, 10^{-6} Meter
MW	=	Molecular Weight
nBEI (nhaBEI)	=	Binding Efficiency Index Based on Non-Hydrogen Atoms = $pKi + Log[nha]$ nha = Number of Non-Hydrogen Atoms
nM	=	Nanomolar, 10^{-9} Molar
nm	=	Nanometer, 10^{-9} Meter
ns	=	Nanosecond, 10^{-9} Second
NPOL (N + O)	=	Number of Polar Atoms
NPT	=	Constant Number of Atom, Pressure, Temperature
NSEI	=	Binding Efficiency Index Based on Polar Surface Area = $\frac{pKi}{NPOL}$ nTDOF = Number of Torsional Degrees of Freedom
NVT	=	Constant Number of Atom, Volume, Temperature
PDB	=	Protein Data Bank pKi = - LogKi
PME	=	*Particle-Mesh-Ewald*
ps	=	Picosecond, 10^{-12} Second
QM	=	Quantum Mechanics
RDF	=	Radial Distribution Function
Rg	=	Radius of Gyration
RMSD	=	Root-Mean-Square Deviation
RMSF	=	Root-Mean-Square Fluctuation
SDF	=	Chemical-Data File
SE	=	Standard Error
SMILES	=	The Simplified Molecular-Input Line-Entry System
Smo	=	Smoothened Receptor
SPC	=	Simple Point Charge Water Model
SPDBV	=	Swiss Protein Data Bank Visualizer
nTDOF	=	Numbers of Torsional Degrees of Freedom
Tot-Drift	=	Total drift
TPSA	=	Topological Polar Surface Area
vdW	=	Van Der Waals
VHTS	=	Virtual High-Throughput Screening

AUTHOR CONTRIBUTIONS

Parham J. Kaboli contributed to the research design, practical work, computations, writing of the manuscript and co-developing of the algorithm; Mohammad Bazrafkan developed the algorithm; Patimah Ismail guided the work in the target selection; King-Hwa Ling edited the manuscript, and commented on the research design. All authors had full access to all data produced in the study and take responsibility for its integrity and accuracy.

ETHICS APPROVAL AND CONSENT TO PARTICIPATE

Not applicable.

HUMAN AND ANIMAL RIGHTS

No Animals/Humans were used for studies that are base of this research.

CONSENT FOR PUBLICATION

Not applicable.

CONFLICT OF INTEREST

The authors declare no conflict of interest, financial or otherwise.

ACKNOWLEDGEMENTS

Authors would like to appreciate Professor Dr. Johnson Stanslas, Pharmatherapeutics Laboratory, UPM, for his gifted cells, and Professor Dr. Celerino Abad-Zapatero, at the University of Illinois at Chicago, Center for Biomolecular Sciences, Department of Medicinal Chemistry and Pharmacognosy, for his book and his new concepts of binding efficiency indices. The authors also thank Ms. Pooja Terasha Stanslas, the managing editor at Everest Communications and Research, for editing the manuscript.

SUPPLEMENTARY MATERIAL

Supplementary material is available on the publisher's website along with the published article.

- The full list of 485 berberine derivatives with molecular parameters.

- Excel-formatted result file of all calculated docking parameters.
- Developed script.

AVAILABILITY OF DATA

Data resulted from molecular modelling and molecular dynamics simulations, and the script developed for automated drug discovery are available on the online version of this article.

REFERENCES

[1] Zhang X, Harrington N, Moraes RC, Wu M-F, Hilsenbeck SG, Lewis MT. Cyclopamine inhibition of human breast cancer cell growth independent of Smoothened (Smo). Breast Cancer Res Treat 2009; 115: 505-21.

[2] Ruat M, Hoch L, Faure H, Rognan D. Targeting of smoothened for therapeutic gain. Trends Pharmacol Sci 2014; 35: 237-46.

[3] Brastianos PK, Horowitz PM, Santagata S, Jones RT, McKenna A, Getz G, *et al*. Genomic sequencing of meningiomas identifies oncogenic SMO and AKT1 mutations. Nat Genet 2013; 45(3): 285-9.

[4] Kubo M, Nakamura M, Tasaki A, Yamanaka N, Nakashima H, Nomura M, *et al*. Hedgehog signaling pathway is a new therapeutic target for patients with breast cancer. Cancer Res 2004; 6071-4.

[5] Tas, S. Use of cyclopamine for the treatment of basal cell carcinoma and other tumors. DE60113733 (**2006**).

[6] Xie J. Implications of hedgehog signaling antagonists for cancer therapy. Acta Biochim Biophys Sin (Shanghai). 2008; 40: 670-80.

[7] Dessole G, Branca D, Ferrigno F, Kinzel O, Muraglia E, Palumbi MC, *et al*. Discovery of *N*-[(1-aryl-1H-indazol-5-yl)methyl]amides derivatives as smoothened antagonists for inhibition of the hedgehog pathway. Bioorganic Med Chem Lett 2009; 19: 4191-5.

[8] Malancona S, Altamura S, Filocamo G, Kinzel O, Hernando JIM, Rowley M, *et al*. Identification of MK-5710((8aS)-8a-methyl-1,3-dioxo-2-[(1*S*,2*R*)-2-phenylcyclopropyl]-N-(1-phenyl-1H-pyrazol-5-yl)hexahydroimid azo[1,5-a]pyrazine-7(1H)-carboxamide), a potent smoothened antagonist for use in Hedgehog pathway dependent malignancies, Part. Bioorganic Med Chem Lett 2011; 21: 4422-8.

[9] Lu W, Geng D, Sun Z, Yang Z, Ma H, Zheng J, *et al*. Scaffold hopping approach to a new series of smoothened antagonists. Bioorganic Med Chem Lett 2014; 24: 2300-4.

[10] Ontoria JM, Bufi LL, Torrisi C, Bresciani A, Giomini C, Rowley M, *et al*. Identification of a series of 4-[3-(quinolin-2-yl)-1,2,4-oxadiazol-5-yl]piperazinyl ureas as potent smoothened antagonist hedgehog pathway inhibitors. Bioorganic Med Chem Lett 2011; 21: 5274-82.

[11] Yang Y-S, Li Q-S, Sun S, Zhang Y-B, Wang X-L, Zhang F, *et al*. Design, modification and 3D QSAR studies of novel 2,3-dihydrobenzo[b][1,4]dioxin-containing 4,5-dihydro-1H-pyrazole derivatives as inhibitors of B-Raf kinase. Bioorg Med Chem 2012; 20: 6048-58.

[12] Ishii T, Shimizu Y, Nakashima K, Kondo S, Ogawa K, Sasaki S, *et al*. Inhibition mechanism exploration of investigational drug TAK-441 as inhibitor against Vismodegib-resistant Smoothened mutant. Eur J Pharmacol 2014; 723: 305-13.

[13] Wang J, Mook RA, Lu J, Gooden DM, Ribeiro A, Guo A, *et al*. Identification of a novel Smoothened antagonist that potently suppresses Hedgehog signaling. Bioorganic Med Chem 2012; 20: 6751-7.

[14] Williams JA, Guicherit OM, Zaharian BI, Xu Y, Chai L, Wichterle H, *et al*. Identification of a small molecule inhibitor of the hedgehog signaling pathway: effects on basal cell carcinoma-like lesions. Proc Natl Acad Sci USA 2003; 100: 4616-21.

[15] Chen JK, Taipale J, Young KE, Maiti T, Beachy PA. Small molecule modulation of Smoothened activity. Proc Natl Acad Sci. USA 2002; 99:14071-6.

[16] Chen JK, Taipale J, Cooper MK, Beachy PA. Inhibition of hedgehog signaling by direct binding of cyclopamine to Smoothened service Inhibition of Hedgehog signaling by direct binding of cyclopamine to Smoothened. Genes Dev 2002; 2743-8.

[17] Li HX, Zeng JF, Shen K. PI3K/AKT/mTOR signaling pathway as a therapeutic target for ovarian cancer. Cancer Epidemiol 2016; 40:152-7.

[18] Burness CB. Sonidegib: First Global Approval. Drugs. Springer International Publishing; 2015; 75:1559-66.

[19] Steg AD, Katre AA, Bevis KS, Ziebarth A, Dobbin ZC, Shah MM, *et al*. Smoothened antagonists reverse taxane resistance in ovarian cancer. Mol Cancer Ther 2012; 11: 1587-97.

[20] Didier Rognan and Isabelle Mus-Veteau. Three-Dimensional Structure of the Smoothened Receptor: Implications for Drug Discovery. Top Med Chem 2015; 16: 127-46.

[21] Wang C, Wu H, Evron T, Vardy E, Han G., Huang X., *et al*. Structural basis for Smoothened receptor modulation and chemoresistance to anticancer drugs. 2014; 5: 4355.

[22] Amakye D, Jagani Z, Dorsch M. Unraveling the therapeutic potential of the Hedgehog pathway in cancer. 2013; 19: 1410-22.

[23] Sekulic A, Migden MR, Oro AE, Dirix L, Lewis KD, Hainsworth JD, *et al*. Efficacy and Safety of Vismodegib in Advanced Basal-Cell Carcinoma. N Engl J Med. 2012; 366: 2171-9.

[24] Lyons TG, O'Kane GM, Kelly CM. Efficacy and safety of vismodegib: a new therapeutic agent in the treatment of basal cell carcinoma. Expert Opin. Drug Saf. 2014; 13: 1125-32.

[25] Rudin CM, Hann CL, Laterra J, Yauch RL, Callahan C a, Fu L, *et al*. Treatment of medulloblastoma with hedgehog pathway inhibitor GDC-0449. N Engl J Med 2009; 361:1173-8.

[26] Brinkhuizen T, Reinders MG, van Geel M, Hendriksen AJL, Paulussen ADC, Winnepenninckx VJ, *et al*. Acquired resistance to the Hedgehog pathway inhibitor vismodegib due to smoothened mutations in treatment of locally advanced basal cell carcinoma. J Am Acad Dermatol 2014; 71: 1005-8.

[27] Buonamici S, Williams J, Morrissey M, Wang A, Guo R, Vattay A, *et al*. Interfering with resistance to smoothened antagonists by inhibition of the PI3K pathway in medulloblastoma. Sci Transl Med 2010; 2: 51ra70.

[28] Wang J, Peng Y, Liu Y, Yang J, Ding N, Tan W. Berberine, a natural compound, suppresses Hedgehog signaling pathway activity and cancer growth. BMC Cancer 2015; 15: 595.

[29] Lin, W.-Y., Wang, P.-L., Lin, C.-M., Tseng P.-Y. Berberine formulations and uses thereof. WO2015095640 (**2014**).

[30] Morris, Goodsell DS, Halliday RS, Huey R, Hart WE, Belew RK, *et al*. Automated docking using a Lamarckian genetic algorithm and an empirical binding free energy function. J Comput Chem 1998; 19: 1639-62.

[31] Morris G, Huey R. AutoDock4 and AutoDockTools4: Automated docking with selective receptor flexibility. J Comput Chem 2009; 30: 2785-91.

[32] Shakil S. A simple click by click protocol to perform docking. EXCLI J 2013; 831-57.

[33] Pujadas G, Vaque M, Ardevol A, Blade C, Salvado MJ, Blay M, *et al*. Protein-ligand docking: a review of recent advances and future perspectives. Curr Pharm Anal 2008; 4: 1-19.

[34] Sudha KN, Shakira M, Prasanthi P, Sarika N, Kumar CN, Babu PA. Virtual screening for novel COX-2 inhibitors using the ZINC database. Bioinformation 2008; 2: 325-9.

[35] Zhang S, Kumar K, Jiang X, Wallqvist A, Reifman J. DOVIS: an implementation for high-throughput virtual screening using AutoDock. BMC Bioinformatics. 2008; 9: 126.

[36] Selick, H.E., Korzekwa, K.R., Mackarehtschian, K. Drug rescue by redesign of ADMET/PK properties. US20030073069 (**2003**).

[37] Benight, A.S., Riccelli, P.V., Hopfinger, A.J., Pancoska P. Modular computational models for predicting the pharmaceutical properties of chemical compunds. US20060136186 (**2002**).

[38] Hiremath, CN. Method for predicting ADMET properties using Abbreviated Profile of Drugs (A-POD). US20130117000 (**2013**).

[39] Houghton, M., Tuszynski, JA., Barakat, K., Mohamed, A. Systems and methods of selecting compounds with reduced risk of cardiotoxicity. WO2015085432 (**2015**).

[40] Abad-Zapatero C. Ligand efficiency indices for drug discovery: Towards an atlas-guided paradigm: Elsevier Science; 2013. Academic Press, eBook ISBN: 9780124046825, Paperback ISBN: 9780124046351.

[41] Kaboli PJ, Bazrafkan M, Ismail P, Ling K.-H. A novel one-click automated drug discovery tool: a new approach based on binding efficiency indices. FASEB J 2017; 31: Suppl 818.7.

[42] Berman HM, Westbrook J, Feng Z, Gilliland G, Bhat TN, Weissig H, Shindyalov IN. The protein data bank. Nucleic Acids Res 2000; 28: 235-42.

[43] Lundborg M, Lindahl E. Automatic GROMACS topology generation and comparisons of force fields for solvation free energy calculations. J Phys Chem B 2015; 119: 810-23.

[44] Peters EAJF, Goga N, Berendsen HJC. stochastic dynamics with correct sampling for constrained systems. J Chem Theory Comput 2014; 10: 4208-20.

[45] Martonák R, Laio A, Parrinello M. Predicting crystal structures: the Parrinello-Rahman method revisited. Phys Rev Lett 2003; 90: 75503.

[46] Yadav IS, Nandekar PP, Shrivastava S, Sangamwar A, Chaudhury A, Agarwal SM. Ensemble docking and molecular dynamics identify knoevenagel curcumin derivatives with potent anti-EGFR activity. Gene 2014; 539: 82-90.

[47] Pettersen EF, Goddard TD, Huang CC, Couch GS, Greenblatt DM, Meng EC, *et al*. UCSF Chimera--a visualization system for exploratory research and analysis. J Comput Chem 2004; 25: 1605-12.

[48] Ma H, Lu W, Sun Z, Luo L, Geng D, Yang Z, *et al*. Design, synthesis, and structure-activity-relationship of tetrahydrothiazolopyridine derivatives as potent smoothened antagonists. Eur J Med Chem 2015; 89: 721-32.

[49] Kasper M, Jaks V, Fiaschi M, Toftgård R. Hedgehog signalling in breast cancer. Carcinogenesis 2009; 30: 903-11.

[50] Peukert S, Miller-Moslin K. Small-molecule inhibitors of the hedgehog signaling pathway as cancer therapeutics. ChemMedChem. 2010; 5: 500-12.

[51] Kaboli PJ, Ismail P, Ling K-H. Berberine derivatives as multi-kinase inhibitors of map kinase and PI3K pathways: molecular modelling, molecular dynamics simulations, and *in vitro* evaluation. FASEB J 2017; 31: (Suppl 1) 671-712

[52] Kaboli PJ, Rahmat A, Ismail P, Ling K-H. Targets and mechanisms of berberine, a natural drug with potential to treat cancer with special focus on breast cancer. Eur J Pharmacol 2014; 740: 584-95.

[53] Onishi H, Katano M. Hedgehog signaling pathway as a therapeutic target in various types of cancer. Cancer Sci 2011; 102: 1756-60.